Pergamon

Journal of Structural Geology, Vol. 16, No. 9, pp. 1233 to 1241, 1994

0191-8141/94 $07.00+0.00

0191-8141(93)E0023-E

Rb/Sr dating of differentiated cleavage from the upper Adelaidean metasediments at Hallett Cove, southern Adelaide fold belt

SIMON TURNER,* MIKE SANDIFORD, THOMAS FLÖTTMANN and JOHN FODEN

Department of Geology and Geophysics, University of Adelaide GPO Box 498, Adelaide, SA 5001, Australia

(*Received* 18 *May* 1993; *accepted in revised form* 19 *November* 1993)

Abstract—Upper Adelaidean psammites from the foreland part of the Late Proterozoic Adelaide fold belt at Hallett Cove have suffered one major deformation which produced upright folds that plunge gently south. Axial to these folds is a well developed differentiation cleavage inferred to have resulted from constant volume, plane-strain deformation by solution transfer and now defined by alternating P- (phyllosilicate-rich) and Q- (quartz-rich) domains. Geochemical analyses show that cleavage development resulted in a 2–4-fold fractionation of Rb/Sr between the P- and Q-domains; thus the age of deformation is datable and isotopic analyses show the P- and Q-domains form a 531 ± 32 Ma isochron. This age is statistically older than the pervasive deformation and metamorphism in the more interior parts of the fold belt, inferred from intrusive ages to have occurred at 485 ± 6 Ma, and thus suggests that deformation either propagated across the fold belt from external to interior zones or that it occurred episodically. The age data allow, but do not demand, that cleavage formation predated the deposition of the overlying Cambrian Kanmantoo Group sediments (<526 Ma). This would lend support to a model in which deposition of the Kanmantoo Group occurred after the onset of convergent deformation in this fold belt.

INTRODUCTION

ANALYSIS of ancient mountain belts and the development of orogens requires, amongst other things, a knowledge of the mechanisms and timing of deformation. Often while the relative timing of deformation events can be determined from fabric relationships, the absolute age of deformation is only indirectly constrained by the ages of associated, deformed and non-deformed, igneous rocks (which may provide minimum rather than maximum ages of deformation). Such ages have so far provided important information on the timing of deformation in the Adelaide fold belt. Here we investigate the development of differentiated cleavage in Late Proterozoic psammites at Hallett Cove and show the resultant fractionation in Rb/Sr within individual beds can be used to date the age of cleavage formation. This represents the first direct dating of deformation in the Adelaide fold belt and the results may have important implications for its tectonic evolution.

GEOLOGICAL SETTING AND BACKGROUND

The Late Proterozoic–Early Cambrian Adelaide fold belt extends through most of the length of South Australia with equivalent sequences in western Tasmania (Williams 1978) and in north Victoria Land, Antarctica (Laird & Grindley 1982) leading various authors (e.g. Ballie 1985) to propose an originally contiguous fold belt along the eastern margin of Gondwanaland. Both temporally and spatially the Adelaide fold belt occupies an important position between the craton to the west and the outboard Phanerozoic Tasman orogen to the east (e.g. Coney *et al.* 1990). The Late Proterozoic (~850–600 Ma), Adelaidean sediments of the fold belt were deposited in relatively shallow water environments developed in probable intracratonic rifts in Archaean–Mid-Proterozoic basement material (see Preiss 1987 for review) and were accompanied by tholeiitic flood basalt volcanism (Crawford & Hilyard 1990). In the southeastern parts of the fold belt, Cambrian sedimentation began with the Cambrian Normanville Group which contains the Truro volcanics (Forbes *et al.* 1972, Van der Stelt 1990). Overlying either the Normanville Group, which is only locally preserved, or elsewhere the Adelaidean is the Kanmantoo Group which consists of an apparently thick (up to 8 km) pile of rapidly deposited flysch-like sediments (Daily & Milnes 1973). Isotope data indicate that these sediments represent mixtures of basement detritus and reworked Adelaidean material (Turner *et al.* 1993). Recent zircon dating on a tuffaceous layer in the upper Normanville Group places the beginning of this last sedimentation episode at 526 ± 4 Ma (Cooper *et al.* 1990).

The Adelaidean, Normanville and Kanmantoo sequences were deformed by the Cambro-Ordovician Delamerian Orogeny (Thompson 1969, Daily *et al.* 1976, Parker 1986). In the southerly exposed sections of the fold belt this involved crustal thickening and Buchan-style metamorphism (see Jenkins & Sandiford 1992 for a recent summary). Orogenic magmatic activity commenced with early mafic dykes and volcanics (Liu & Fleming 1990, Turner & Foden 1990) subsequently followed by I- and S-type granite plutonism (Foden *et al.* 1990, Sandiford *et al.* 1992). The cessation of deformation was associated with a late-orogenic suite of

*Current address: Department of Earth Sciences, Open University, Milton Keynes MK7 6AA, U.K.

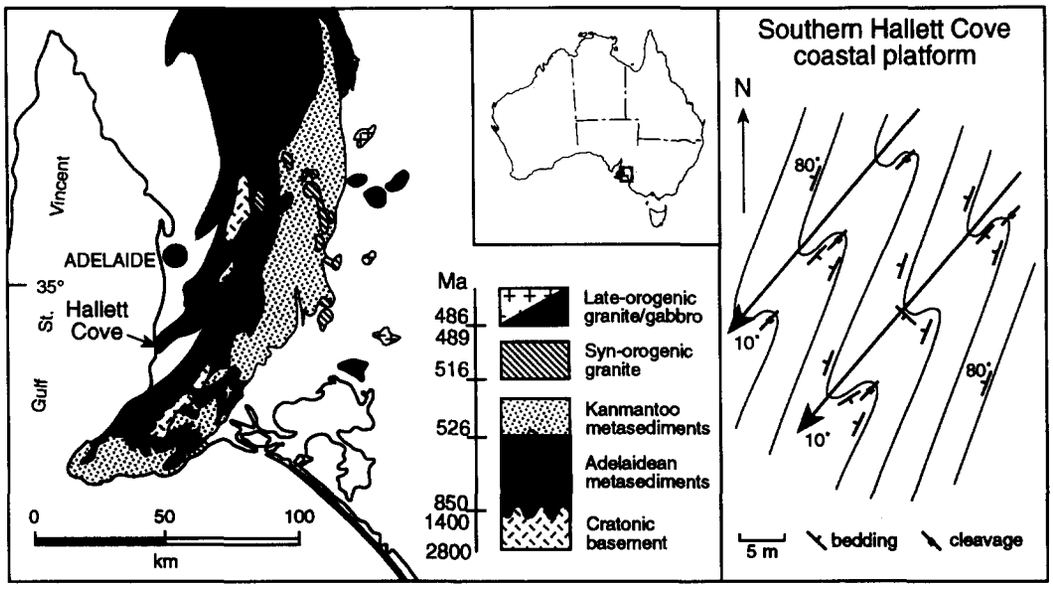

Fig. 1. Geological map of the southern Adelaide fold belt showing the principal sedimentological and igneous stratigraphy with the geochronology in the legend based on Foden *et al.* (submitted), Cooper *et al.* (1992) and Webb *et al.* (1983). Metamorphic grade and structural intensity are greatest around the syn-orogenic granites. The right-hand part of the map is a sketch of the structural relationships within the Adelaidean sequence in the southern part of Hallett Cove.

undeformed A-type granites and gabbroic intrusives (Foden *et al.* 1990, Sandiford *et al.* 1992, Turner *et al.* 1992a) as well as an inferred 15 km of uplift and erosion (Turner *et al.* 1993) and may therefore reflect thinning of the lithospheric mantle (e.g. Turner *et al.* 1992b). The ages of these deformed (516 ± 4 Ma to 485 ± 6 Ma) and undeformed (486 ± 5 Ma) granites so far provide the main chronologic framework for the orogeny (Foden *et al.* submitted).

The principal elements and geochronology of the southern Adelaide fold belt are depicted in Fig. 1. The overall structure is that of a large antiform which plunges gently south and at least one, usually upright, deformational fabric is observable in most areas. Thrust faults which may duplicate parts of the sequence dip to the southeast (Jenkins 1986, 1990, Flöttmann & James 1992, Flöttmann *et al.* 1992). The Adelaidean sequences have suffered low-temperature, low-pressure metamorphism whereas the Kanmantoo Group, which forms the eastern edge of outcrop (Fig. 1), reached upper amphibolite grade with local development of kyanite–sillimanite assemblages (e.g. Offler & Fleming 1968, Mancktelow 1979, Sandiford *et al.* 1990, 1992). These high metamorphic grades are associated with polyphase structural fabrics and migmatites (Fleming & White 1984) centred around a thermal core resulting from (and demarcated by) the intrusion of the syn-orogenic I- and S-type granites (Fig. 1). Zircon ages from associated, deformed and undeformed intrusives indicate that the dominant deformation and metamorphism at this eastern margin of the fold belt occurred at 485 ± 6 Ma (Foden *et al.* submitted).

The sedimentary sequences of the fold belt have long been thought to represent a semi-continuous history of deposition during protracted extension (e.g. Preiss 1987) while the intercalation of the Normanville Group with the mafic Truro Volcanics and the turbiditic nature of the Kanmantoo Group has led to a general belief that these sediments were deposited in a developing rift (e.g. Von der Borch 1980, Parker 1986). However, such logic might be questioned in light of the short time span between the onset of Kanmantoo deposition at 526 Ma and intrusion of the earliest deformed granite plutons about 516 Ma, a limited time for both deposition of the Kanmantoo Group and reversal of the tectonic regime from extensional basin to convergent orogen. Clearly, further constraints on the timing of onset of convergent deformation relative to deposition and magmatism are critical to these arguments and the development of tectonic models for the Adelaide fold belt.

STRUCTURAL RELATIONSHIPS AT HALLETT COVE

The structural geometry of the southern Adelaide fold belt shows clear characteristics of a foreland fold thrust belt (cf. Jenkins 1990). Displacement was west-northwest (cratonward) directed as indicated by slip lineations and the long axis-orientation of elongated conglomerate and tillite clasts which mark the X-axis of the finite strain ellipsoid ($X > Y > Z$). The youngest exposed Adelaidean strata occur in the western part of the fold belt. Deformation intensity increases towards the east where thrust slices may also involve slivers of Middle Proterozoic basement and deformation is manifested in pervasively strained phyllonitic zones which are dominated by gently ESE-dipping transposition fabrics. The geology at Hallett Cove is well documented (Talbot & Nesbitt 1968) and belongs to the less intensely deformed structural foreland of the southern Adelaide fold belt. This structural domain is characterized by large-scale open folds, which are part of a generally foreland-

dipping sequence. Contrasting to the pervasive strain further east, Delamerian deformation in the foreland is characterized structurally by subvertically oriented, spaced cleavage (Fig. 2a).

Exposure along the coastal platform at Hallett Cove consists of folded Brachina Formation psammites from the (Late Proterozoic) upper Adelaidean sequences of the Adelaide fold belt (Fig. 1). The rocks have undergone only very low-grade (sub-greenschist facies) metamorphism and one major deformation event, producing upright folds which plunge gently south. Individual beds are ~5–15 cm thick and, in general, dip steeply to the west forming the western limb of an anticline which plunges gently (~10°) southwest concordant with the regional structure. In the hinges of small parasitic folds, beds have a near horizontal attitude, with the plunge of these folds being approximately parallel to the overall anticline (Fig. 1). Approximately axial planar to these folds is a near vertical cleavage which, within individual beds, consists of a well developed differentiated cleavage defined by alternating P- (phyllosilicate-rich) and Q- (quartz-rich) domains (terminology after Stephens *et al.* 1979, Waldron & Sandiford 1988), corresponding to dark and light banding in hand specimen (Fig. 2a). Best developed in the axial regions of the parasitic folds, individual P- and Q-domains reach up to 2 and 4 cm in width, respectively, with the P-domains being volumetrically subordinate to the Q-domains in all cases. This fabric clearly truncates sedimentary bedding with P-domains being generally quite sharply defined and sometimes forming an anastomosing network. In thin section, bedding is observed to be sharply folded through the P-domains (Fig. 2a & b).

PETROGRAPHY AND CLEAVAGE FORMATION

The cleavage is an axial planar fabric which has involved horizontal differentiation, within individual, initially homogeneous beds, into P- and Q-domains. In thin section, P- and Q-domains are distinguished by the relative proportions of constituent minerals, particularly phyllosilicates and quartz. Bedding is well defined by bands of heavy minerals which lie at a high angle to the P–Q fabric whereas P-domains form around folds in the bedding (Fig. 2b). The compositional differences are manifest in the differing modal ratio of quartz to phyllosilicate as revealed by back-scattered electron images (Fig. 2c). The P-domains consist of quartz set in a matrix of mixed muscovite and clay minerals such as illite. Q-domains predominantly contain quartz along with some clay minerals, rare albite and minor apatite. Unfortunately, more detailed probe identification of the phyllosilicate mineralogy is hindered by the extremely fine grain size which resulted in most analyses being multiphase composites.

The microstructures of the P- and Q-domains are also distinctive (Fig. 2c). Q-domains are dominated by quartz which is often angular and detrital along with minor muscovite, illite and altered albite. These domains show little evidence of any fabric though some elongate quartz grains are aligned with bedding. In contrast, the P-domains are typified by a predominance of elongate phyllosilicates with a strong preferred orientation defining the P–Q fabric, perpendicular to bedding (Fig. 2c). Quartz and opaques in the P-domain are elongated in alignment with the P–Q fabric while the centre of the P-domains is often fractured (Fig. 2b). Individual quartz grains show corrosion and pressure shadows suggesting that the principal axis of shortening was parallel to bedding and that maximum extension was in the plane of the P–Q fabric (Fig. 2c). The alignment of phyllosilicates in the Q-domain, semi-parallel to bedding (at a high angle to the P–Q fabric) compared with those in the P-domains (parallel to the P–Q fabric) suggests growth and rotation within a stress field. An important point is that, being perpendicular to bedding, the compositional differences between the P- and Q-domains reflect physico-chemical differentiation associated with fabric formation rather than initial inhomogeneities in the sediment beds.

Differentiation cleavage like that described here has been discussed at length in the literature (e.g. Beach 1979, Stephens *et al.* 1979, Rutter 1983, Waldron & Sandiford 1988) and the reader is referred to these studies for detailed discussion of P–Q fabric formation. Waldron & Sandiford (1988) argued that these cleavages develop via constant volume, plane-strain deformation dominated by solution transfer in a stationary fluid. Chemical gradients set up in this intergranular fluid by the imposition of a stress field promote diffusive transfer and chemical fractionation (Rutter 1983). Physical differentiation of the initially homogeneous beds of sediment may also involve mineral reactions and modification of detrital and diagenetic minerals with accumulations of newly crystallized micas, the products of these reactions in the P-domains (Beach 1979). These models all predict considerable chemical fractionation during cleavage formation which we now consider in more detail since this forms the basis for dating the cleavage.

CHEMICAL FRACTIONATION DURING CLEAVAGE FORMATION

At Hallett Cove individual P- and Q-domains are large enough to be separated for chemical analysis. Seven hand specimen sized samples taken within ~10 m of each other were cut into 2 cm thick slabs perpendicular to bedding and the P–Q fabric. The individual P- and Q-domains from selected P–Q pairs were then separated using a small chisel, with the phyllosilicate-rich P-domains easily cleaving from the Q-domains. Once separated, the P- and Q-samples were crushed, hand picked and milled in a tungsten–carbide mill. XRF, accurate Rb, Sr and Sr isotopic analyses were then performed following standard techniques as described in Turner *et al.* (1993).

The differing modal composition of the P- and Q-

domains is evident in their chemical analyses (Table 1). Thus the quartz-rich Q-domains are SiO_2 and Al_2O_3 rich but K_2O poor whilst the phyllosilicate-rich P-domains are enriched in K_2O and Al_2O_3 and depleted in SiO_2. Note that the degree of this contrast differs from sample to sample. Mobile trace elements appear to have behaved like their chemically similar major elements and thus, for example, Rb is enriched in the K-rich P-domains.

Chemical fractionation during cleavage formation can be examined by comparing the concentrations of elements in the P- and Q-domains relative to an immobile element. Stephens *et al.* (1979) and Waldron & Sandiford (1988) have suggested that Zr is chemically inert during cleavage development and in Fig. 3 we have plotted ratios of elements in the P- and Q-domains divided by the same incompatible element (Zr) concentration in each domain much in the manner of Waldron & Sandiford (1988). The elements have been ordered such that those partitioned into the Q-domain are on the left, whilst those partitioned into the P-domain are on the right with the more immobile elements in between. This shows that Pb, Nb, Y and Th have behaved coherently during cleavage development whilst Si, Ti, Na, V, Al, Sr, Fe, Mg, REE, Ga, Ba, Rb and K showed non-coherent behaviour, in other words were mobile during cleavage development. In detail, Si, Ti, Na, Sr, Fe and Mg are partitioned into the Q-domain (or migrated from the P-domain into the Q-domain) while the REE, V, Al, Ga, Ba, Rb and K are partitioned into the P-domain (or migrated from the Q-domain to the P-domain). Elements such as Zr, Nb, Pb, Y and Th are concentrated in phases like zircon which are resistant to dissolution and therefore show coherent behaviour.

For constant volume deformation, the concentration ratio of inert elements, such as Zr, between the P- and Q-domains during cleavage development provides an estimate of the degree of strain, or the amount of shortening. For the samples analysed, the concentration factor for Zr indicates that principal finite shortening was ~30% greater in the P-domains than in the Q-domains.

Rb/Sr ISOTOPES AND THE AGE OF CLEAVAGE DEVELOPMENT

The chemical differentiation during cleavage development has produced marked shifts in the Rb/Sr ratios which range from 0.75 in the Q-domains to 3.35 in the P-domains (Table 2 and Fig. 3). Thus the age of cleavage development should be recorded by Sr isotopes if the sediments were homogeneous with respect to $^{87}Sr/^{86}Sr$ at the sampling scale (tens of metres) at the time of deposition and the only subsequent change was fractionation of Rb/Sr during cleavage development. Four samples spaced over 1000 km along strike of the Bunyeroo Formation (which overlies the Brachina Formation) exhibit remarkable isotopic homogeneity, particularly for Nd isotopes (Turner *et al.* 1993). These data along with the lithological uniformity of the sequence at Hallett Cove when combined with the relatively distal and well-mixed nature of the Brachina Formation sediments provides some encouragement that the sediments were initially homogeneous. In addition, their low metamorphic grade, and the fact that they only exhibit evidence of a single deformation suggest they have not been significantly disturbed since this deformation event. Nevertheless, the best test of these assumptions lies in whether the Sr isotopic data form an isochron and if the initial $^{87}Sr^{86}Sr$ ratio so derived is reasonable. Sr isotopic data for the P- and Q-domains analysed are given in Table 2. Using the measured average $^{87}Sr/^{86}Sr$ and Rb/Sr errors of 0.01 and 1%, respectively, these data form a 14 point isochron with an age of 536 ± 7 Ma (MSWD 20) suggesting the above assumptions hold (Fig. 4). Importantly, the initial $^{87}Sr/^{86}Sr$ ratio (0.71872 ± 0.0006) is within error of the average for pelitic sediments from the upper Adelaidean sequences which is ~0.719–0.720 (Turner *et al.* 1993).

Although fabrics in alpine paragneisses have been similarly dated by Thöni (1988), Rb/Sr whole-rock analyses of low-grade sediments often reflect the age of deposition, but may also reflect the age of their source rocks or a younger structural, metamorphic or diagenetic event (see Faure 1986 for a recent review of Rb/Sr dating of sediments). Since the depositional age of the Brachina Formation is ~601 Ma (Webb *et al.* 1983, Preiss 1987), the isochron obtained from Hallett Cove is not a depositional age, nor is it a source rock age since the basement to the Adelaidean is Archaean to Mid-Proterozoic in age. This basement material would be a likely candidate for the radiogenic end-member if the isochron represented a mixing line, yet the average basement has both lower $^{87}Rb/^{86}Sr$ and $^{87}Sr/^{86}Sr$ (Turner *et al.* 1993) than many of the P-domain analyses. Furthermore, two end-member mixing would produce linear arrays between elements on variation diagrams; however this is not observed as a plot of Sr vs Rb illustrates (Fig. 5). The age is also considered unlikely to reflect metamorphism since the peak of metamorphism in the southern Adelaide fold belt occurred around 485 ± 6 Ma (Foden *et al.* submitted). Consequently the age obtained is believed to be that of cleavage formation although technically speaking it is an errorchron. The MSWD is high probably because the initial sediments were not completely homogeneous at the scale of sampling and there has been some partial resetting towards the dominant thermal event in the eastern part of the fold belt at 485 ± 6 Ma. A model 2 isochron, with MSWD = 1, gives 531 ± 32 Ma and this larger error must be considered more appropriate. However, since weathering removes Sr into seawater (thereby lowering the Rb/Sr ratio of sediments), and the effect of any subsequent metamorphism would be to reset the isotopic system, this age is likely to represent a minimum estimate of the time of fabric formation. In this context, it may be significant that there is growing evidence for similar Middle Cambrian aged deformation in sequences from Antarctica (Rowell *et al.* 1992, Goodge *et*

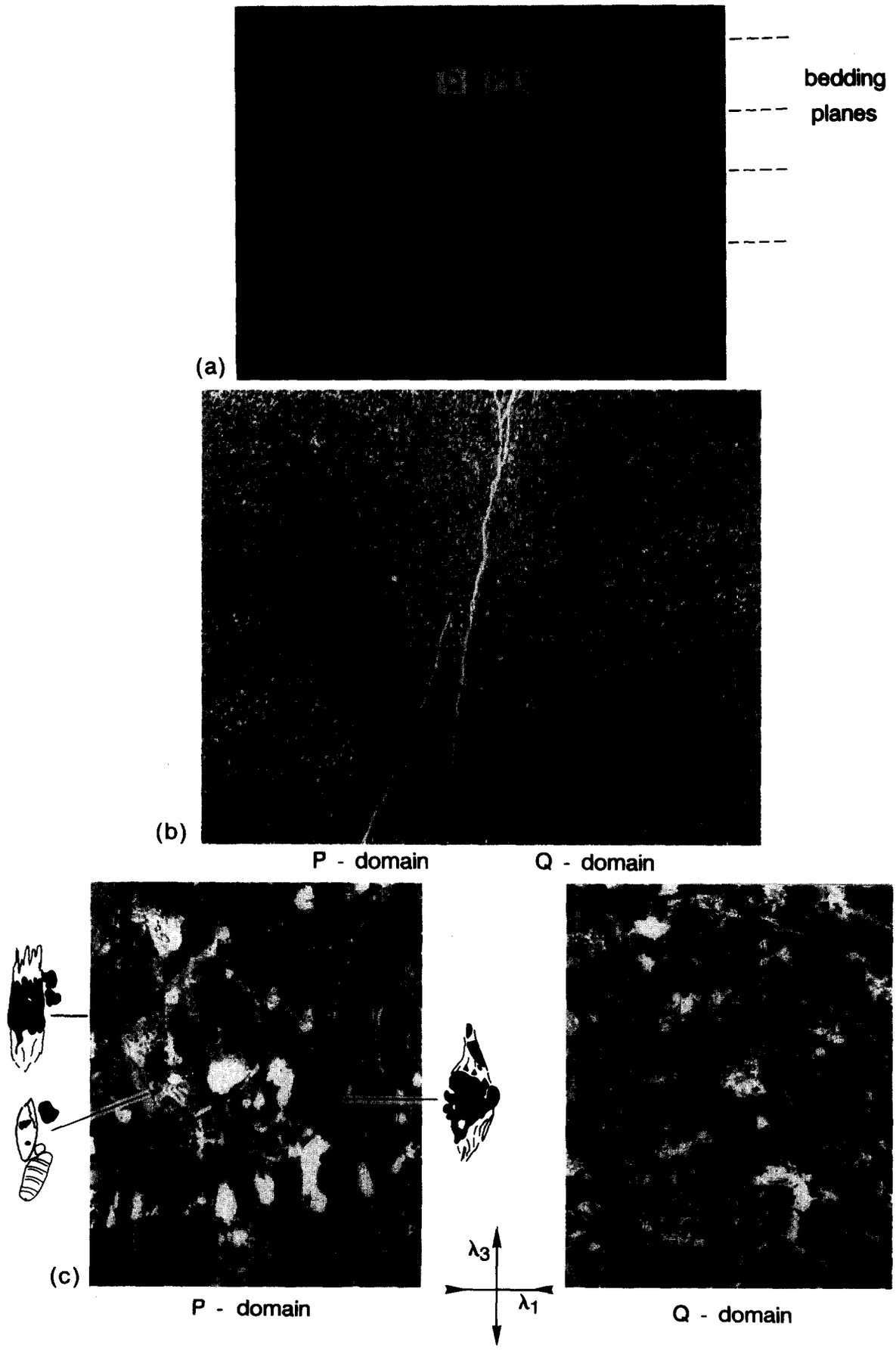

Fig. 2. (a) Field photograph of P–Q fabric at Hallett Cove (the pen is 15 cm long). (b) Photomicrograph of the differentiated cleavage, cut perpendicular to bedding (well defined by heavy mineral bands) and P–Q fabric, showing the axial P- and Q-domains (width of photograph is 2 cm). (c) Back-scattered electron micrographs of P- and Q-domains showing the increased abundance of phyllosilicates (grey) in the P-domain, relative to quartz (black) in the Q-domain (width of photographs is 300 μm). Note the stronger preferred alignment of phyllosilicates, elongate opaques (white) and quartz with pressure shadows (arrowed) in the P-domain.

Table 1. Major and trace element analyses of P- and Q-domains from Hallett Cove

Sample No.	CL-1 P	CL-1 Q	CL-5 P	CL-5 Q	CL-13 P	CL-13 Q	CL-13W P	CL-13W Q	CL-14 P	CL-14 Q	CL-15 P	CL-15 Q	CL-16 P	CL-16 Q
SiO_2	56.96	67.22	57.77	62.27	61.00	63.89	59.04	63.53	61.29	63.27	60.13	64.23	59.62	59.82
TiO_2	1.91	1.54	2.21	1.63	1.75	1.34	2.05	2.18	2.16	1.59	1.87	1.59	1.84	1.95
Al_2O_3	19.53	12.32	17.32	11.93	16.08	14.61	17.58	12.51	16.26	12.71	15.54	13.08	15.92	15.64
Fe_2O_3*	8.05	8.87	9.33	10.17	9.35	8.65	8.56	9.02	8.36	8.58	9.93	10.12	10.12	10.41
MnO	0.02	0.04	0.03	0.12	0.03	0.03	0.03	0.09	0.02	0.12	0.03	0.04	0.03	0.04
MgO	2.30	2.70	2.46	3.41	2.61	2.87	2.71	3.01	2.10	3.12	3.01	3.00	2.79	2.94
CaO	0.63	0.62	0.64	1.64	0.53	0.50	0.51	1.16	0.61	1.58	0.57	0.61	0.61	0.68
Na_2O	2.30	3.10	2.97	3.47	2.52	2.54	2.87	3.38	3.36	3.51	3.36	3.30	3.24	3.25
K_2O	4.09	1.24	3.25	0.96	3.04	2.42	3.33	1.23	2.84	1.13	2.30	1.42	2.56	2.37
P_2O_5	0.44	0.34	0.41	0.30	0.36	0.31	0.32	0.29	0.39	0.30	0.34	0.29	0.33	0.33
LOI	3.37	2.43	3.08	3.86	2.81	2.65	3.03	3.25	2.48	3.74	2.92	2.60	2.85	2.87
Total	99.60	100.42	99.47	99.76	100.08	99.81	100.03	99.65	99.87	99.65	100.00	100.28	99.91	100.30
Cr	47	43	239	276	72	60	68	48	61	48	50	46	51	51
Ni	121	160	47	45	37	38	48	40	44	38	40	40	44	44
Sc	16	10	14	11	19	15	18	12	17	12	15	12	15	16
V	163	105	151	105	162	135	163	121	145	107	134	112	135	139
Pb	19	17	20	17	20	17	18	19	18	15	21	21	25	26
Rb	190.3	60.8	142.0	45.1	138.4	111.3	148.1	58.0	123.7	60.0	105.4	67.7	115.1	107.2
Sr	56.8	55.5	60.4	67.1	53.0	50.5	57.2	61.5	62.4	66.4	62.1	64.2	59.3	59.5
Ba	280	113	212	99	215	177	226	106	179	329	164	127	179	169
Ga	27	16	23	14	22	20	23	15	20	16	20	17	20	20
Nb	28	21	30	22	25	19	27	23	27	20	24	20	24	25
Zr	358	300	356	275	313	225	333	359	368	267	282	249	282	292
Y	54	38	46	35	41	33	39	37	43	32	25	31	36	36
Th	25	18	16	11	16	12	15	12	14	11	11	9	13	12
U	3	2	3	3	2	4	4	2	1	1	1	2	3	2
La	53	39	43	32	47	42	38	29	36	26	33	30	34	33
Ce	105	75	83	60	89	79	74	60	70	53	63	55	60	62
Nd	50	34	41	28	40	36	33	28	35	23	30	27	39	29

*Total iron as Fe_2O_3.

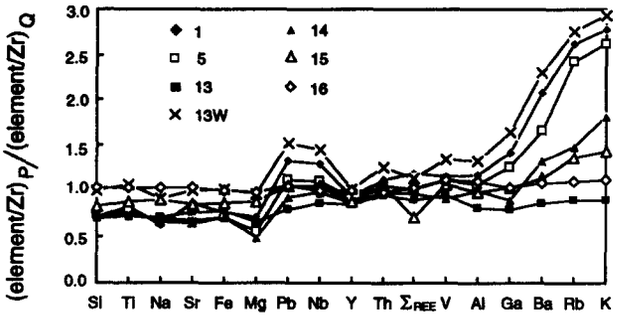

Fig. 3. Ratio plot for various elements (normalized to the immobile element Zr) in the P-domain relative to the Q-domain (see text for discussion). Elements are ordered such that those partitioned into the Q-domain are on the left while those partitioned into the P-domain are on the right. The sample numbers are the same as those in Tables 1 and 2.

al. 1993) that are believed to be contiguous with the Adelaide fold belt (e.g. Flöttmann *et al.* 1993).

IMPLICATIONS FOR THE EVOLUTION OF THE ADELAIDE FOLD BELT

The original intention of this work was to investigate the possibility of using the Rb/Sr system to date differentiated cleavage. The age obtained, however, may have important implications for the evolution of the Adelaide fold belt and so we will briefly discuss these further. Recent mapping and structural analysis shows that the southern Adelaide fold belt sequence contains major thrust faults suggesting east–west convergent displacement (Jenkins 1986, 1990, Flöttmann & James 1992, Flöttmann *et al.* 1992). However, the time of cleavage development at Hallett Cove (531 ± 32 Ma) is statistically older than the dominant deformation and metamorphism at the eastern margin of the fold belt (485 ± 6 Ma) as inferred from zircon ages from associated, deformed and undeformed intrusives (Foden *et al.* submitted). If the available age constraints reflect the changing

Table 2. Rb/Sr isotopic analyses of P- and Q-domains. Details of procedures and blanks are given in Turner *et al.* (1993)

Sample No.	Rb (ppm)	Sr (ppm)	$^{87}Rb/^{86}Sr$	$^{87}Sr/^{86}Sr$
C1-1 P	190.3	56.8	9.703	0.791769 ± 44
CL-1 Q	60.8	55.5	3.175	0.742993 ± 56
CL-5 P	142.0	60.4	6.811	0.768545 ± 50
CL-5 Q	45.1	67.1	1.946	0.733854 ± 58
CL-13 P	138.4	53.0	7.612	0.780021 ± 73
CL-13 Q	111.3	50.5	6.419	0.771652 ± 45
CL-13W P	148.1	57.2	7.546	0.778248 ± 85
CL-13W Q	58.0	61.5	2.738	0.739659 ± 52
CL-14 P	123.7	62.4	5.741	0.761566 ± 55
CL-14 Q	60.0	66.4	2.621	0.739469 ± 38
CL-15 P	105.4	62.1	4.914	0.755283 ± 55
CL-15 Q	67.7	64.2	3.050	0.742414 ± 28
CL-16 P	115.1	59.3	5.624	0.761729 ± 34
CL-16 Q	107.2	59.5	5.224	0.758828 ± 25

Isotope analyses performed at the University of Adelaide on a Finnigan Mat 261 Mass spectrometer (NBS 987 = 0.710183 ± 37).

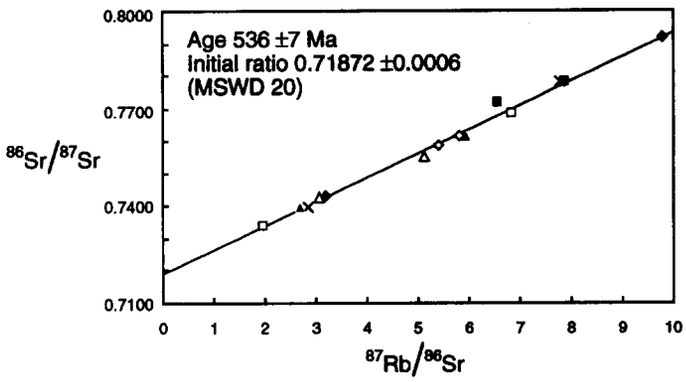

Fig. 4. Rb/Sr isochron for the P- and Q-domains analysed in Tables 1 and 2 ($\lambda = 1.42 \times 10^{-11}$ year^{-1}). Symbols as for Fig. 3.

locus of deformation through time, they imply that deformation migrated from external to interior zones of the fold belt. This is contrary to the widely held belief that deformation propagates towards the foreland. Alternatively the age data may be interpreted to record episodic pulses of contractional deformation during the Delamerian orogeny.

One further possibility that the age data published here allow (but do not demand) is that the onset of deformation within the Adelaidean sequences pre-dated, or was synchronous with, deposition of the Kanmantoo Group (at 526 ± 4 Ma) as suggested by a number of recent authors (e.g. Coney *et al.* 1990, Mancktelow 1990). During convergent deformation, advancing thrust stacks may cause flexural downwarping of the lithosphere providing a trough for sediment deposition (e.g. Laubscher 1978, Beaumont 1981, Jordan 1981, Stockmal *et al.* 1986). Some support for this model is provided by the contact between the Normanville and Kanmantoo Groups as exposed to the south of Adelaide at Carrickalinga Head (Jenkins & Sandiford 1992). Here thin beds of black shale interbedded with carbonate in the upper Normanville Group are overlain by a thick turbiditic succession. This sequence marks a change in basin response involving deepening in the absence of sediment supply followed by the dramatic influx of abundant sediment. As noted by Coney *et al.* (1990) and Jenkins & Sandiford (1992) this would be predicted on emergence of an encroaching thrust stack, and such

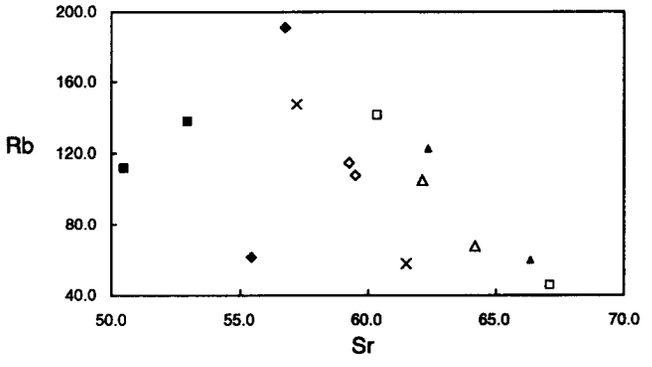

Fig. 5. Plot showing no clear correlation between Sr and Rb for the P- and Q-domains, as expected if the isochron in Fig. 4 were a mixing line or fictitious isochron. Symbols as for Fig. 3.

sedimentary successions, which ultimately become incorporated within the advancing fold-and-thrust belt, may be a hallmark of foreland basins (Hoffman 1987). The isotopic signature of the Kanmantoo Group sediments suggests mixing of reworked Adelaidean sediments and detritus from the cratonic basement (Turner *et al.* 1993) and this is predicted in numerical models of foreland basin development (Jordan 1981, Stockmal *et al.* 1986). Unfortunately, the uncertainty on the age of cleavage development at Hallett Cove precludes confirmation of this second hypothesis.

CONCLUSIONS

In conclusion, differentiation cleavage in low-grade psammites involves fractionation of Rb/Sr allowing direct dating of the time of deformation. In the Adelaide fold belt, data indicate the deformation observed in the foreland sequences at Hallett Cove pre-dated some of that observed in the sequences further to the east. Thus deformation propagated towards the hinterland or occurred in several pulses. The isotopic data would allow this deformation to have pre-dated deposition of the overlying Kanmantoo Group challenging the long held belief that the entire sedimentary sequence was deposited under a single continuous extensional regime, and deposition in a foreland basin may be an alternative. Similar differentiated cleavages are also recorded from the Adelaidean sequences east of Truro (Pisters 1991) and from Torrens Gorge (Talbot & Hobbs 1968) and future Rb/Sr dating of these fabrics may provide further insights into the tectonic evolution of the fold belt.

Acknowledgements—We wish to thank John Stanley for performing the XRF major and trace element analyses and David Bruce for his expert assistance in improving techniques in the isotope laboratory at Adelaide. Simon Kelley, Steve Blake, Chris Adams and an anonymous reviewer are all thanked for helpful discussions and reviews of the manuscript.

REFERENCES

Ballie, P. W. 1985. A Palaeozoic suture in eastern Gondwanaland. *Tectonics* **4**, 653–660.

Beach, A. 1979. Pressure solution as a metamorphic process in deformed terrigenous sedimentary rocks. *Lithos* **12**, 51–58.

Beaumont, C. 1981. Foreland basins. *Geophys. J. R. astr. Soc.* **65**, 291–329.

Coney, P. J., Edwards, A., Hine, R., Morrison, F. & Windrim, D. 1990. The regional tectonics of the Tasman orogenic system, eastern Australia. *J. Struct. Geol.* **12**, 519–543.

Cooper, J. A., Jenkins, R. J. F., Compston, W. & Williams, I. S. 1992. Ion-probe zircon dating of a mid-Early Cambrian tuff in South Australia. *J. geol. Soc. Lond.* **149**, 185–192.

Crawford, A. J. & Hilyard, D. 1990. Geochemistry of Late Proterozoic tholeiitic flood basalts, Adelaide Geosyncline, South Australia. *Spec. Publ. geol. Soc. Aust.* **16**, 49–67.

Daily, B. & Milnes, A. R. 1973. Stratigraphy, structure and metamorphism of the Kanmantoo Group (Cambrian) in its type section east of Tunkallilla Beach, South Australia. *Trans. R. Soc. S. Aust.* **97**, 213–242.

Daily, B., Firman, J. B., Forbes, B. G. & Lindsay, J. M. 1976. Geology. In: *Natural History of the Adelaide Region* (edited by Twidale, C. R. *et al.*). *R. Soc. S. Aust.* 17–18.

Faure, G. 1988. *Principles of Isotope Geology*. Wiley, New York.

Foden, J. D., Turner, S. P. & Morrison, R. S. 1990. The tectonic implications of Delamerian magmatism in South Australia and western Victoria. *Spec. Publ. geol. Soc. Aust.* **16**, 465–482.

Forbes, B. G., Coates, R. P. & Daily, B. 1972. Truro Volcanics. *Q. Geol. Notes, Geol. Surv. S. Aust.* **44**, 1–5.

Fleming, P. D. & White, A. J. R. 1984. Relationships between deformation and melting in the Palmer migmatites. *Aust. J. Earth Sci.* **31**, 351–360.

Flöttmann, T. & James, P. R. 1992. Tectonic evolution of the southern Adelaide fold belt: a strain and balanced-section approach. *Geol. Soc. Aust. Abs.* **32**, 241.

Flöttmann, T., James, P. R., Johnson, T. & Rogers, J. 1992. Fault and shear zone minor- and micro-structures and fabrics associated with large scale thrusting in the Talisker area of the southern Fleurieu Peninsula, South Australia. *Geol. Soc. Aust. Abs.* **32**, 231–232.

Flöttmann, T., Gibson, G. M. & Kleinschmidt, G. 1993. Structural continuity of the Ross and Delamerian orogens of Antarctica and Australia along the margin of the palaeo-Pacific. *Geology* **21**, 319–322.

Goodge, J. W., Walker, N. W. & Hansen, V. L. 1993. Neoproterozoic–Cambrian basement involved orogenesis within the Antarctic margin of Gondwana. *Geology* **21**, 37–40.

Hoffman, P. F. 1987. Early Proterozoic foredeeps, foredeep magmatism, and Superior-type iron formations of the Canadian Shield. In: *Proterozoic Lithospheric Evolution* (edited by Kroner, A). *Am. Geophys. Un. Geodyn. Ser.* **17**, 85–99.

Jenkins, R. J. F. 1986. Ralph Tate's enigma–and the regional significance of thrust faulting in the Mt Lofty Ranges. *Geol. Soc. Aust. Abs.* **15**, 101.

Jenkins, R. J. F. 1990. The Adelaide Foldbelt: tectonic reappraisal. *Spec. Publ. geol. Soc. Aust.* **16**, 396–420.

Jenkins, R. J. F. & Sandiford, M. 1992. Observations on the tectonic evolution of the southern Adelaide fold belt. *Tectonophysics* **214**, 27–36.

Jordan, T. E. 1981. Thrust loads and foreland basin evolution, Cretaceous, western United States. *Bull. Am. Ass. Petrol. Geol.* **65**, 2506–2520.

Laird, M. G. & Grindley, G. W. 1982. Antarctica. *Spec. Publ. geol. Soc. Aust.* **9**, 17–22.

Laubscher, H. P. 1978. Foreland folding. *Tectonophysics* **47**, 325–337.

Liu, S. F. & Fleming, P. D. 1990. Mafic dykes and their tectonic setting in the southern Adelaide Foldbelt, South Australia. In: *Mafic Dykes and Emplacement Mechanisms* (edited by Parker, A. J. *et al.*). Balkema, Rotterdam, 401–413.

Mancktelow, N. S. 1979. The structure and metamorphism of the southern Adelaide fold belt. Unpublished Ph.D. thesis, University of Adelaide.

Mancktelow, N. S. 1990. The structure of the southern Adelaide fold belt, South Australia. *Spec. Publ. geol. Soc. Aust.* **16**, 215–229.

Offler, R. & Fleming, P. D. 1968. A synthesis of folding and metamorphism in the Mt. Lofty Ranges, South Australia. *J. geol. Soc. Aust.* **15**, 245–266.

Parker, A. J. 1986. Tectonic development and metallogeny of the Kanmantoo trough in South Australia. *Ore Geol. Rev.* **1**, 203–212.

Pisters, D. 1991. Isotopic plateau variations within marbles: an example from the Milendella Limestone, South Australia. Unpublished Hons. thesis, University of Adelaide.

Preiss, W. V. 1987. The Adelaide Geosyncline—Late Proterozoic stratigraphy, sedimentation, palaeontology and tectonics. *Bull. geol. Surv. S. Aust.* **53**.

Rowell, A. J., Rees, M. N. & Evans, K. R. 1992. Evidence of major Middle Cambrian deformation in the Ross orogen, Antarctica. *Geology* **20**, 31–34.

Rutter, E. H. 1983. Pressure solution in nature, theory and experiment. *J. geol. Soc. Lond.* **140**, 725–740.

Sandiford, M., Oliver, R. L., Mills, K. J. & Allen, R. V. 1990. A cordierite–staurolite–muscovite association, east of Springton, Mt Lofty Ranges; implications for the metamorphic evolution of the Kanmantoo Group. *Spec. Publ. geol. Soc. Aust.* **16**, 483–495.

Sandiford, M., Foden, J., Zhou, S. & Turner, S. 1992. Granite genesis and the mechanics of convergent orogenic belts with application to the Southern Adelaide fold belt. *Trans. R. Soc. Edinb.* **83**, 83–93.

Stephens, M. B., Glasson, M. G. & Keays, R. R. 1979. Structural and chemical aspects of metamorphic layering development in metasediments from Clunes, Australia. *Am. J. Sci.* **279**, 129–160.

Stockmal, G. S., Beaumont, C. & Boutilier, R. 1986. Geodynamic models of convergent margin tectonics: transition from rifted margin to overthrust belt and consequences for foreland-basin development. *Bull. Am. Ass. Petrol. Geol.* **70**, 181–190.

Talbot, J. L. & Hobbs, B. E. 1968. The relationship of metamorphic differentiation to other structural features at three localities. *J. Geol.* **76**, 581–587.

Talbot, J. L. & Nesbitt, R. W. 1968. The Hallett Cove area. In: *Geological Excursions in the Mount Lofty Ranges and Fleurieu Peninsula.* McGraw Hill, Sydney, 18–26.

Thöni, M. 1988. Rb–Sr isotopic resetting in mylonites and pseudotachylites: Implications for the detachment and thrusting of the Austroalpine basement nappes in the eastern Alps. *Jb. Geol. B.-A.* **131**, 169–201.

Thompson, B. P. 1969. The Kanmantoo Group and Early Palaeozoic tectonics. In: *Handbook of South Australian Geology* (edited by Parkin, L. W.). *Geol. Surv. S. Aust.*, 97–108.

Turner, S. P. & Foden, J. D. 1990. The nature of mafic magmatism through the evolution of the Adelaide Foldbelt and subsequent Delamerian Orogeny. In: *Mafic Dykes and Emplacement Mechanisms* (edited by Parker, A. J. *et al.*). Balkema, Rotterdam, 431–434.

Turner, S. P., Foden, J. D. & Morrison, R. S. 1992a. Derivation of some A-type magmas by fractionation of basaltic magma: an example from the Padthaway Ridge, South Australia. *Lithos* **28**, 151–179.

Turner, S. P., Sandiford, M. & Foden, J. D. 1992b. Some geodynamic and compositional constraints on "postorogenic" magmatism. *Geology* **20**, 931–934.

Turner, S. P., Foden, J. D., Sandiford, M. & Bruce, D. 1993. Sm–Nd isotopic evidence for the provenance of sediments from the Adelaide fold belt and southeastern Australia with implications for episodic crustal addition. *Geochim. cosmochim. Acta* **57**, 1837–1857.

Van der Stelt, B. J. 1990. The geochemistry, petrology and tectonic setting of the Truro Volcanics. Unpublished Hons. thesis, University of Adelaide.

Von der Borch, C. C. 1980. Evolution of Late Proterozoic to Early Palaeozoic Adelaide Foldbelt, Australia: comparisons with post-Permian margins. *Tectonophysics* **70**, 115–134.

Waldron, H. M. & Sandiford, M. 1988. Deformation volume and cleavage development in metasedimentary rocks from the Ballarat slate belt. *J. Struct. Geol.* **10**, 53–62.

Webb, A. W., Coats, R. P., Fanning, C. M. & Flint, R. B. 1983. Geochronological framework of the Adelaide Geosyncline. *Geol. Soc. Aust. Abs.* **10**, 7–9.

Williams, E. 1978. Tasman fold belt system in Tasmania. *Tectonophysics* **48**, 159–205.